DESIGN 2022

Design Rules for Laser Beam Melted Particle Dampers

T. Ehlers ✉ and R. Lachmayer

Leibniz Universität Hannover, Germany

✉ ehlers@ipeg.uni-hannover.de

Abstract

By means of additive manufacturing, especially laser powder bed fusion, particle dampers can be integrated locally into structural components and thus significantly reduce component vibrations. However, detailed design recommendations for additively manufactured particle dampers do not yet exist. The research question in this paper is: How can the effect of particle damping be described as a function of excitation force, cavity width and cavity length? For beams made of AlSi10Mg, it is shown that a powder-filled cavity of 2.5% to 5% is sufficient to increase the damping by more than x10.

Keywords: additive manufacturing, design guidelines, lightweight design, functional integration, particle damping

1. Introduction

Additive manufacturing is characterised by a high degree of design freedom (Yang *et al.*, 2015; Lachmayer *et al.*, 2017). For product design, this results in a number of advantages, such as the production of components with a high degree of complexity or the possibility to realise components with a high degree of functional integration (Yang *et al.*, 2015; Ehlers *et al.*, 2020). Additive manufacturing is already being used profitably for topology-optimised and flow-optimised components in particular, as numerous methods and tools are available for design (Reiher, 2019; Wiberg *et al.*, 2019; Kumke, 2018). However, the potential of additive manufacturing has not yet been exhausted for dynamically highly loaded components (Ehlers *et al.*, 2021; Scott-Emuakpor *et al.*, 2018).

As a result of increased sustainability requirements, which are more and more being tightened by politics, lightweight design plays a decisive role (Wurst *et al.*, 2022; Lachmayer and Lippert, 2020). However, components designed for lightweight construction are increasingly prone to component vibrations, which have to be reduced by elaborate measures (Hanselka, 2001). In order to reduce vibrations, additional mass must often be added to the system, which is in contradiction to lightweight design.

Particle dampers are a simple and effective measure for reducing vibrations in the field of lightweight design (Lu *et al.*, 2017; Scott-Emuakpor *et al.*, 2021). Using additive manufacturing, especially powder bed-based processes such as laser powder bed fusion (LPBF), particle-filled cavities can be integrated into the component in one manufacturing step, thus addressing the effect of particle damping (Künneke and Zimmer, 2017; Ehlers and Lachmayer, 2020). This makes it possible to reduce component vibrations by more than a factor of 20 in some cases (Schmitz *et al.*, 2020; Ehlers *et al.*, 2021; Ehlers and Lachmayer, 2022; Scott-Emuakpor *et al.*, 2019). Furthermore, it is possible to solve the conflict between high stiffness and high damping at the same time, since the powder-filled cavities can be integrated in the area of the neutral fibre (Ehlers and Lachmayer, 2021). Sometimes it is also referred to as "damping for free", since the integration of the particle damper hardly increases the mass or the costs of components that are additively manufactured anyway (Ehlers *et al.*, 2021). In addition, the cavities should be integrated in the area of highest deflection in order to maximise the damping (Lu *et al.*, 2017;

ENGINEERING DESIGN PRACTICE

2443

Hollkamp and Gordon, 1998). It turns out that areas of high deflection and high stresses are often locally separated from each other, so that the integration of a particle-filled cavity has little influence on the component strength. For example, for a cantilever beam for the first vibration mode, the maximum amplitudes occur at the free end and the highest stresses occur in the clamping. This shows that a separate design for strength and damping can be pursued. Figure 1 shows an exemplary manufacturing process of laser beam melted particle dampers using the example of a damped gear wheel.
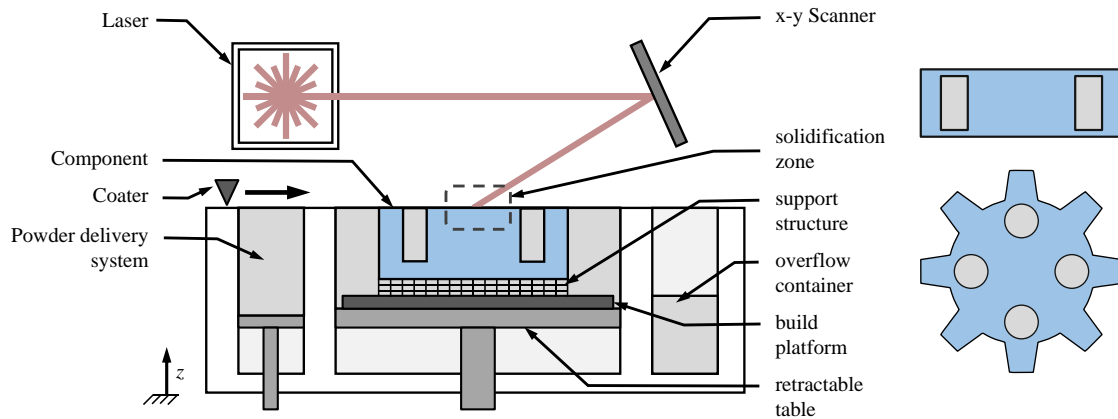

Figure 1. Laser powder bed fusion of a particle damped gear (Ehlers *et al.*, 2021)

The effect of particle damping is not yet fully understood due to numerous design parameters and the high non-linearities. The relevant design parameters include, for example, the excitation force, excitation frequency, particle mass, packing density, dimensions of the cavities, etc. For example, a cylindrical cavity results in more broadband damping than a cuboid cavity, for the same cavity size. (Künneke and Zimmer, 2021). For this reason, there are still no design tools and only isolated methodological approaches for the design of additively manufactured particle dampers. Up to now, it is known that the energy in the system when using particle dampers is dissipated via combined loss mechanisms from impacts and friction between the particles themselves and with the walls of the cavity. A schematic representation is shown in Figure 2.
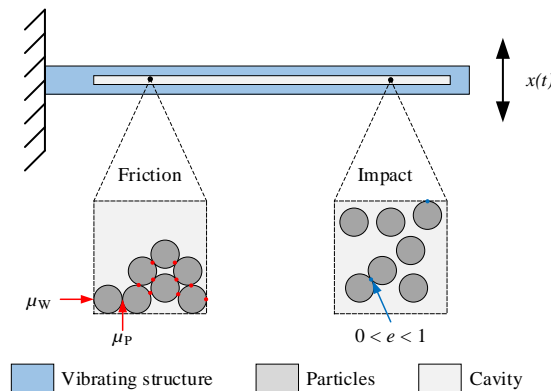

Figure 2. Schematic diagram of an additive manufactured particle damper (Ehlers and Lachmayer, 2022)

The main advantages of particle dampers include broadband damping under harsh environmental conditions ranging from heavy contamination to extreme operating temperatures, low wear and, as a result, increased component service life (Lu *et al.*, 2017; Papalou and Masri, 1996; Saeki, 2005).
Current research approaches in the field of additive manufacturing focus on describing the effect of particle damping on test specimens in order to derive corresponding design rules on this basis (Künneke and Zimmer, 2021; Ehlers *et al.*, 2021; Scott-Emuakpor *et al.*, 2019; Schmitz *et al.*, 2020). However, these design rules are underpinned by too few studies and in some cases no detailed design curves can be derived for the investigated parameters because too few support points have been used.

The aim of this paper is to derive detailed conclusions on particle damping as a function of the excitation force, the cavity height and the cavity length. Compared to previous work from the state of the art, significantly more support points (six support points) are investigated for the cavity geometry. This number of support points is intended to better capture the non-linear influence. For the characterisation of the damping effect, beams made of the aluminium alloy AlSi10Mg are selected as test geometry and excited to vibrate from 10 N to 100 N by means of an automated impulse hammer. The focus of the evaluation is on the first beam bending mode. As a result of this paper, design curves for damping as a function of excitation force, cavity length and cavity height are available. From the design curves it can be derived at which cavity length or cavity volume a saturation of the damping occurs and a further enlargement of the cavity does not provide a significant added value to increase the damping.

2. Experimental methodology

In the following, the methodical procedure for characterising the effect of particle dampers is presented and builds on the preliminary work from (Ehlers *et al.*, 2021; Ehlers and Lachmayer, 2022). A design of experiments (DoE) is selected as the methodological procedure, as the simulative design is challenging due to the high degree of non-linearities. The design space is exploratively investigated on cuboid beams with dimensions of 20 x 20 x 200 mm³. These external dimensions determine the natural frequency to a large extent, which has a strong influence on the effect of particle damping. These dimensions should not be varied in order to minimise the experimental effort, so that the results presented here only apply to a narrow frequency range. However, on this basis, detailed statements can be made about the damping curve over the cavity height and cavity length and a standard 3^k test plan can be selected in further work. For the 3^k test plan, the damping curve determined here can be used for interpolation between the support points, thus minimising the test effort. The particle-filled cavity of the beams is designed as a cuboid and manufactured horizontally so that support structures in the cavity can be dispensed with (see Figure 3).
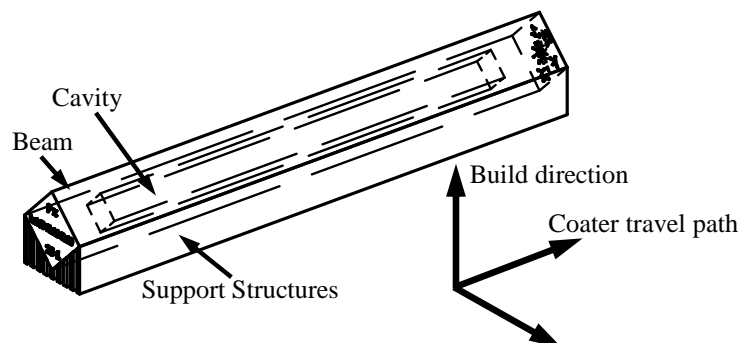

Figure 3. Schematic representation of a particle filled beam on the building platform (Ehlers and Lachmayer, 2022)

For the characterisation of the particle damper effect, both the influences of the cavity height and the cavity length are characterised by six support points. The cavity height is analysed from 0 % to 25 % in 5 % steps and the cavity length in the interval [0 %, 2.5 %, 5 %, 10 %, 15 %, 20 %]. All cavity geometries have in common that they are positioned centrally in the beam. In addition to the geometric parameters, the excitation force from 10 N to 100 N in steps of 10 N and the influence of anistotropy are also investigated in the test. The influence of anisotropy is analysed by exciting the beams to vibrate in the *y* and *z* directions.

For the clear assignment and orientation of the beams during the test, the beam number and a coordinate system are printed on the front surfaces of all beams. The following notation is used:

- *x*-direction: Coater travel path
- *y*-direction: Perpendicular to coater travel path
- *z*-direction: Build direction

Previous experiments with beams made of AlSi10Mg have shown that the standard deviation of the damping of 3 printed beams of the same topology is low (Ehlers *et al.*, 2021), so that only one beam per parameter is produced in the following.

The beams were produced in 5 batches, although not all batches are considered in this paper. It should be noted here that not all parameters are numbered consistently, as not all printed beams are analysed in this paper. However, with regard to research data management and comparison with other works, this numbering leads to a clear and consistent allocation. The final test plan is shown in Table 1.

Table 1. Test plan

Parameter	Batch	outer beam dimensions in mm			Cavity dimensions in mm			Cavity in %
		Length	Height	Width	Width	Height	Length	
1	1	200	20	20	Full material			
22	4	200	20	20	10	7.5	160	15
23	4	200	20	20	10	5	160	10
24	4	200	20	20	10	2.5	160	5
25	4	200	20	20	10	10	160	20
26	4	200	20	20	10	12.5	160	25
27	5	200	20	20	10	10	160	20
28	5	200	20	20	10	10	120	15
29	5	200	20	20	10	10	80	10
30	5	200	20	20	10	10	40	5
31	5	200	20	20	10	10	20	2.5

2.1. Machine and process parameter

The beams are made of the aluminium alloy AlSi10Mg, as this alloy has a high performance index and is therefore suitable as a lightweight material. According to Ashby, the performance index indicates the ratio of component stiffness to component mass (Ashby and Cebon, 1993). The EOS M280 LPBF system with the standard parameters for the AlSi10Mg alloy is used as the production system. These include above all the layer thickness of 30 μm. The average grain size D50 of the powders was 47 μm for the aluminium alloy. The aluminium alloy supports are removed from the build platform with a saw. The support structures of the aluminium components could be broken off and no subsequent heat treatment is applied to the beams. Subsequently, all components were sandblasted. In addition, the mass of all beams was measured in order to draw conclusions about the particulate mass.

2.2. Experimental setup

The laboratory setup for characterising the damping is shown in Figure 4. The beams, supported on foam, are excited to vibrate by an automated pulse hammer (5800SL by Dytran) and the response signal is measured by an accelerometer (M353B17 by PCB Piezotronics). The VibRunner by m+p international is used as the data acquisition device, which records the time data and calculates the frequency response functions (FRF). This type of experimental setup is preferred because there is no parasitic friction in the clamping point of the beam, as would be the case, for example, with excitation using a shaker. In addition, the automation of the impulse hammer allows a high degree of reproducibility to be achieved, which could not be achieved by hand. The beams are then excited to vibrate from two sides in order to characterise the influence of the production-related anisotropy. This is particularly essential for characterising the damping in the case of non-square cross-sections of the cavity, as is the case when varying the cavity height. A positive side effect is that the influence of the cavity width is quantified and no new beams need to be fabricated.

In order to be able to characterise the influence of the excitation force, the beams are excited to vibrate from 10 N to 100 N in 10 N steps and the damping in the frequency range is evaluated using the circle-fit method. Corresponding calculation principles for the circle-fit method can be found in

(Ewins, 2000). Furthermore, it has already been shown in Ehlers et al. that this test setup including the evaluation method can be successfully used to characterise the effect of particle damping (Ehlers *et al.*, 2021).
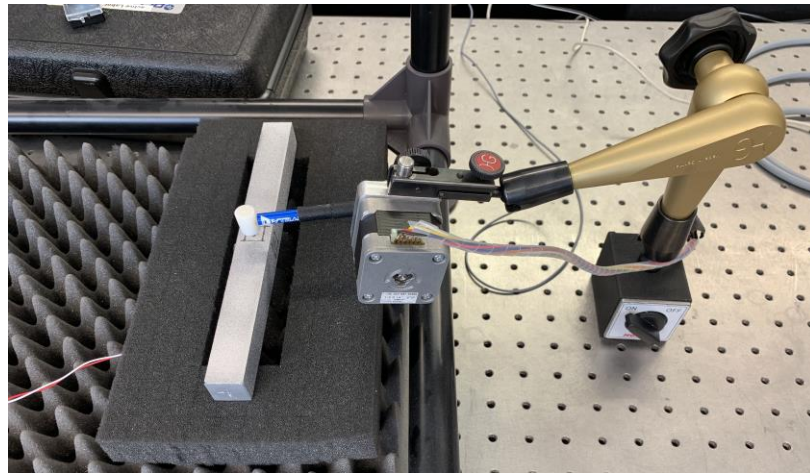

Figure 4. Test setup for the characterization of particle damping (Ehlers *et al.*, 2021)

3. Results

To better interpret the results of the particle damper effect, the particle mass and packing density of the beams are first determined by measuring all beams with a scale. Then the particle mass can be calculated using equation 1.

$$m_{P,x} = m_x - \frac{m_0}{V_0} \times V_x \qquad (1)$$

The beam volumes V_x and V_0 are determined from CAD and the masses m_x and m_0 of the printed beams are measured with a scale. The index 0 indicates that it is the fully-fused (solid) beam with the same external dimensions as the beam under investigation. Packing density η can finally be determined by the ratio of densities ρ, see equation 2.

$$\eta_x = \frac{\rho_{P,x}}{\rho_0} \quad \text{with} \quad \rho_{P,x} = \frac{m_{P,x}}{V_0 - V_x} \qquad (2)$$

Here $\rho_{P,x}$ represents the density of the particles in the cavity. Density of the particles is approximated to be equal to that of the fused material. In addition, manufacturing deviations lead to a difference between theoretical and real volume. Another influence may be the local porosity. Table 2 shows the results for beam mass, particle mass and packing density.

Table 2. Beam mass m_B, particle mass m_P and packing density η of the beams

Parameter	1	Variation of cavity width					Variation of cavity length				
		22	23	24	25	26	27	28	29	30	31
Cavity size [%]	1	15	10	5	20	25	20	15	10	5	2.5
m_B [g]	212.20	197.5	197.6	206.6	193.1	188.5	193.4	197.8	202.1	206.8	209
m_P [g]	0	17.1	6.6	5.0	23.3	29.4	23.6	17.4	11.1	5.2	2.06
η [%]	1	53.66	31.20	47.22	54.88	55.33	55.58	54.76	52.40	49.10	38.74

3.1. Damping characteristics as a function of cavity height and excitation force

The results of the particle damper effect as a function of cavity height and excitation force are presented below (parameter 1, 22-26). Due to the limitations of the accelerometer, only forces up to 100 N can be analysed. Figure 5 shows these results for an excitation in *y*-direction and Figure 6 for an excitation in *z*-direction. The force-dependent curve is approximated for each cavity size by a separate hyperbolic

ENGINEERING DESIGN PRACTICE

function, see also (Ehlers *et al.*, 2021), where a cavity of 0 % denotes the fully-fused beam (parameter 1). The individual force-dependent curves are linearly connected, resulting in a 3D plot. Figures 5 and 6 show that the damping decreases with increasing excitation force and reaches a plateau at 100 N. This plateau is particularly relevant for the design, as the damping should rather be assumed too low than too high, so that the focus of the result description is placed on high forces.
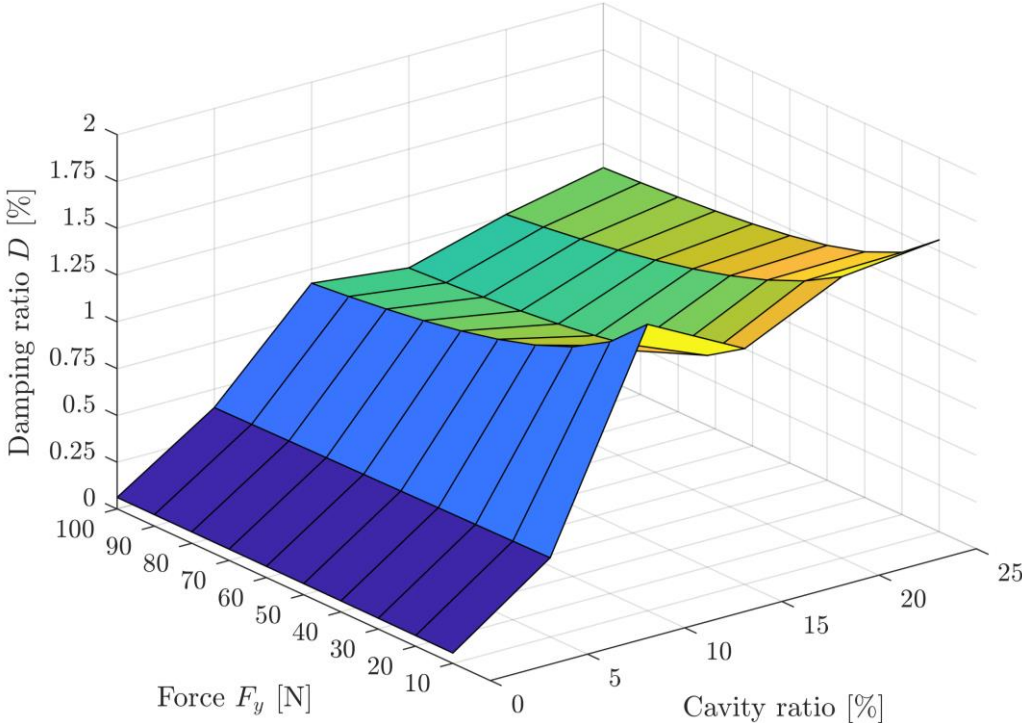

Figure 5. Damping characteristics as a function of the cavity height and the excitation force F_y
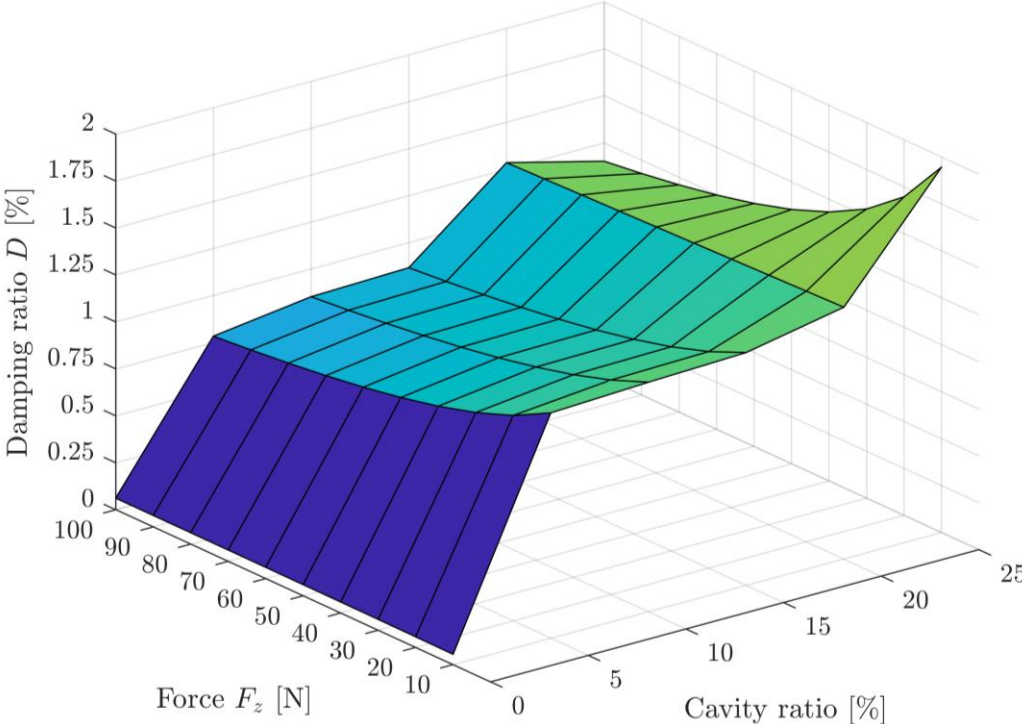

Figure 6. Damping characteristics as a function of the cavity height and the excitation force F_z

Figure 5 shows that no significant increase in damping occurs above a cavity size of 10 %, where approximately 1 % damping is achieved. The mean value of the damping of the fully-fused beams in the y-direction is $D_z = 0.053$ % and in the z-direction $D_y = 0.066$ %. Thus, for a cavity size of 10 %, an excitation in the y-direction results in an increase in damping by a factor of 15. The mean value of the natural frequency of the fully-fused beams for an excitation in the y-direction is $f_{0,y} = 2640.0$ Hz and for an excitation in the z-direction is $f_{0,z} = 2668.6$ Hz. For the particle-damped beams, the natural frequency increases with increasing cavity volume up to 2714 Hz for a cavity size of 20 %.

For excitation in the z-direction (Figure 6), there is a similar gain in damping (factor 14) for as little as 5 % cavity volume. It becomes clear that the excitation direction (in y or z direction) seems to have a decisive influence with a ratio of cavity height to cavity width of 4:1.

It is noticeable in this measurement campaign that the packing density from Table 2 is not constant for parameters 22 to 25. The packing density increases with increasing cavity volume, except for parameter 24.

3.2. Damping characteristics as a function of cavity length and excitation force

The results of the particle damper effect as a function of cavity length and excitation force are presented below (parameter 1, 27-31). Due to the limitations of the accelerometer, only forces up to 100 N can be analysed here. Figure 7 shows these results for an excitation in the y-direction and Figure 8 for an excitation in the z-direction. The force-dependent curve is also approximated here for each cavity size by a separate hyperbolic function and the individual force-dependent curves are connected linearly. Figures 7 and 8 show that the damping decreases with increasing excitation force and reaches a plateau at 100 N. In the following, the focus is also placed on the description of the damping at high forces.

In Figure 7, already for an excitation in y-direction from a cavity size of 2.5 %, approx. 75 % of the damping is realised, which is present for a cavity size of 15 % or 20 %. However, it is noticeable that the damping here is slightly lower than in Figures 5 and 6. Figure 8 differs from Figure 7 in that the damping at a cavity of 2.5 % is only half as high.
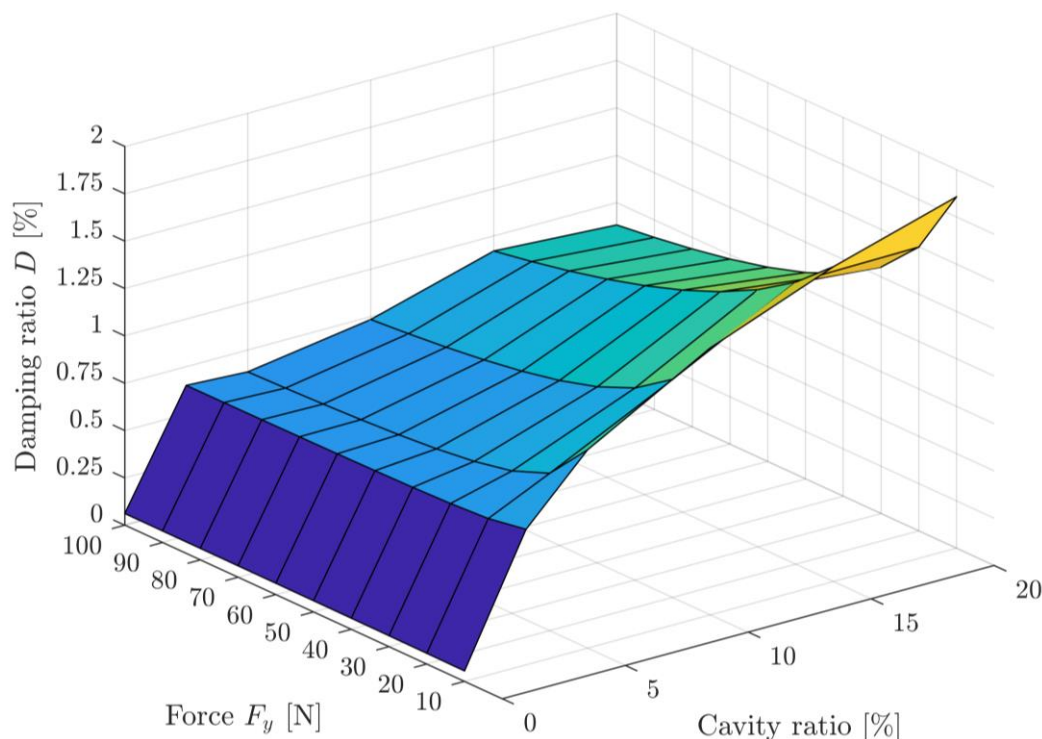

Figure 7. Damping characteristics as a function of the cavity length and the excitation force F_y
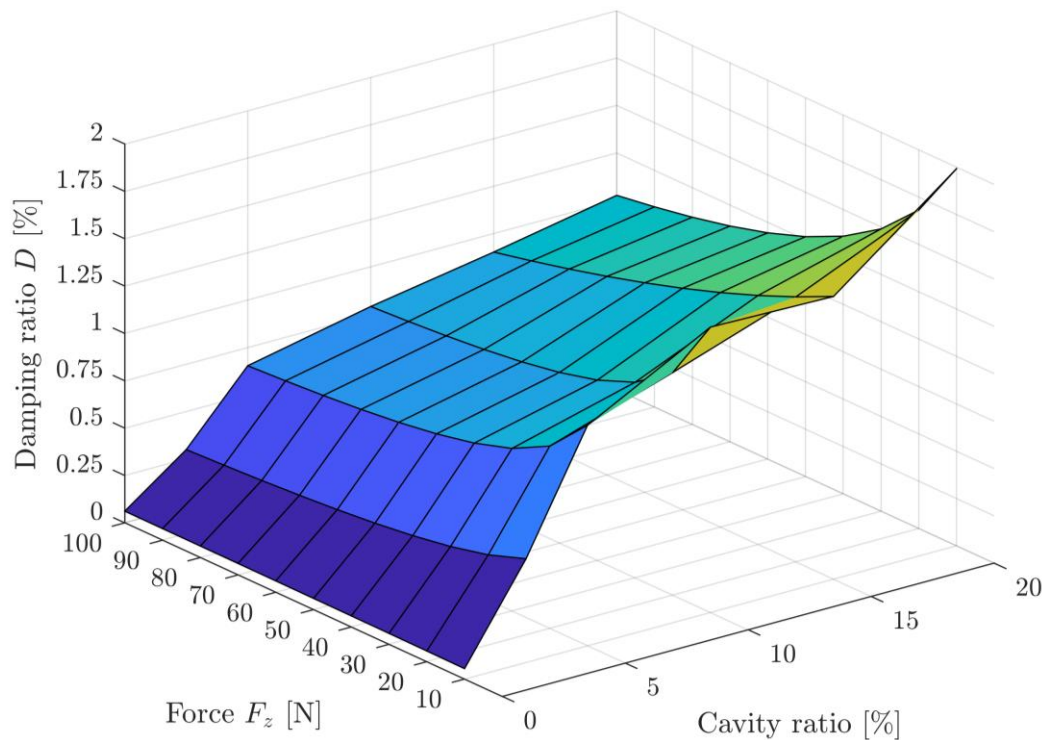
Figure 8. Damping characteristics as a function of the cavity length and the excitation force F_z

For Figures 7 and 8 it can be seen that no significant increase in damping occurs above a cavity size of 10 %, where approximately 1 % damping is achieved. For the particle-damped beams, the natural frequency also increases here with increasing cavity volume up to 2725 Hz at a cavity size of 20 %.

It is noticeable that the packing density from Table 2 for parameters 22 to 25 increases with increasing cavity size.

3.3. Reproducibility and error consideration

The standard deviations of the damping curves, which are not shown in Figures 5 to 8 for clarity, are of the same order of magnitude. The values of the standard deviations increase from the small cavity to the large cavity. Furthermore, the values of the standard deviation vary by approx. 10 % in relation to the force-dependent damping curves. Furthermore, it could be shown in preliminary work, in which three beams per parameter were manufactured, that the production-related deviations of the dampings lie between 10 % and 15 % (Ehlers *et al.*, 2021).

Thus, it can be stated for this test setup that a relative error of 10 % to 15 % should be considered. This is particularly relevant for the robust design of additively manufactured particle dampers.

4. Discussion

This paper shows for the first time a detailed investigation of the effect of particle damping as a function of excitation force, anisotropy, cavity height and cavity length for a large number of support points. It has been shown that the plateau of the damping for high forces can be used to make detailed statements on the influence of cavity height and cavity length. It is noticeable that the damping no longer increases significantly above a cavity size of 10 % and that a cavity size of 2.5 % to 5 % can already be sufficient to reduce component vibrations by a factor of 10 to 15.

Especially for small cavities of ≤ 5 %, the use of a smaller cavity length is preferable to a small cavity cross-section for the same cavity volume due to the lower direction-dependent damping properties. When varying the cavity height, it is noticeable for small cavities (5 %) that the damping is strongly direction-dependent, since the cavity height is 4x smaller than the cavity width. It was noticed that the damping is worse in the *y*-direction, although the dimension is larger in the *y*-direction. One explanation could be that the narrow cross-

section in the direction of vibration causes the particles to interlock with the wall. In the other spatial direction (*z*), the cross-section in the direction of vibration is larger, so that the risk of the particles interlocking and the path being blocked is minimised.

With the design recommendation that large cavity cross-sections and small cavity lengths should be used, however, it must be taken into account that only the first bending mode was evaluated in this test setup. At higher modes, the positions of the local maxima of the vibration response shift. Since the positioning of the cavities should always be in the area of the highest deflection, a continuous cavity with a smaller cavity height could prove to be more effective when damping more than one mode. Otherwise, several cavities with a small cavity length would have to be integrated.

Another point that makes the transferability of the results difficult is that the damping values also depend on the excitation frequency, see (Ehlers *et al.*, 2021). Accordingly, these values only apply to frequencies between 2500 Hz and 2800 Hz, where an error between 10 % and 15 % is to be expected. However, these findings can be used to minimise the experimental effort in further investigations by no longer having to use a large number of support points for the characterisation of the damping and by using a 3^k experimental design with only three support points. Between the support points, the damping curve characterised here could be used for interpolation. Especially when varying the cavity length, it would be sufficient to produce and characterise only beams with a cavity of 5 % and 20 %. These detailed damping results could also be used to validate mechanical models. Although the component damping could be significantly increased, the influence on the component service life must also be investigated in further work, as the rough surface can be a crack indicator for dynamically loaded components.

5. Conclusion

The effect of particle damping could be characterised for beams made of AlSi10Mg with dimensions of 20 x 20 x 200 mm³ as a function of the excitation force, cavity height, cavity length and anisotropy. The force-dependent damping could be investigated in steps of 10 N from 10 N to 100 N. The results show that a plateau occurs. It is shown that a plateau is reached from forces of 100 N and the course of the damping can be assumed to be constant at high forces. Particularly with large aspect ratios between the cavity width and the cavity height, direction-dependent properties in the damping could be determined. The damping was higher when the smaller dimension of the cross-section points in the direction of vibration. For a small cavity, an increase in damping of more than a factor of 10 could be demonstrated from 2.5 % to 5 % cavity volume. For smaller cavities, a small cavity length with a large cavity cross-section is preferable for the same cavity volume. In further work, these results will be used to design a motorcycle triple clamp under the aspects of high stiffness and damping with low mass at the same time. Furthermore, the parameter fields presented here serve to validate mechanical substitute models.

References

Ashby, M.F. and Cebon, D. (1993), "Materials selection in mechanical design", Le Journal de Physique IV, Vol. 03 No. C7, C7-1-C7-9. http://dx.doi.org/10.1051/jp4:1993701.

Ehlers, T. and Lachmayer, R. (2020), "Einsatz additiv gefertigter Partikeldämpfer – eine Übersicht", in Lachmayer, R., Rettschlag, K. and Kaierle, S. (Eds.), Konstruktion für die Additive Fertigung 2019, Springer Berlin Heidelberg, Berlin, Heidelberg, pp. 123–142. http://dx.doi.org/10.1007/978-3-662-61149-4_9.

Ehlers, T. and Lachmayer, R. (2021), "Design of a Motorcycle Triple Clamp Optimised for Stiffness and Damping", in Pfingstl, S., Horoschenkoff, A., Höfer, P. and Zimmermann, M. (Eds.), Proceedings of the Munich Symposium on Lightweight Design 2020, Springer Berlin Heidelberg, Berlin, Heidelberg, pp. 1–17. http://dx.doi.org/10.1007/978-3-662-63143-0_1.

Ehlers, T. and Lachmayer, R. (2022), "Design of Particle Dampers for Laser Powder Bed Fusion", Applied Sciences, Vol. 12 No. 4. http://dx.doi.org/10.3390/app12042237.

Ehlers, T., Lachmayer, R., Vajna, S. and Halle, T. (2020), "Producibility", in Vajna, S. (Ed.), Integrated Design Engineering, Springer International Publishing, Cham, pp. 287–323. http://dx.doi.org/10.1007/978-3-030-19357-7_9.

Ehlers, T., Tatzko, S., Wallaschek, J. and Lachmayer, R. (2021), "Design of particle dampers for additive manufacturing", Additive Manufacturing, Vol. 38, p. 101752. http://dx.doi.org/10.1016/j.addma.2020.101752.

Ewins, D.J. (2000), Modal testing: Theory, practice and application, Mechanical engineering research studies Engineering dynamics series, Vol. 10, 2. ed., Research Studies Press, Baldock.

Hanselka, H. (2001), "Adaptronics as a Key Technology for Intelligent Lightweight Structures", Advanced Engineering Materials, Vol. 3 No. 4, pp. 205–215. http://dx.doi.org/10.1002/1527-2648(200104)3:4<205::AID-ADEM205>3.0.CO;2-H.

Hollkamp, J.J. and Gordon, R.W. (1998), "Experiments with particle damping", in Davis, L.P. (Ed.), Smart Structures and Materials 1998: Passive Damping and Isolation, Sunday 1 March 1998, San Diego, CA, SPIE, pp. 2–12. http://dx.doi.org/10.1117/12.310675.

Kumke, M. (Ed.) (2018), Methodisches Konstruieren von additiv gefertigten Bauteilen, Springer Fachmedien Wiesbaden, Wiesbaden. http://dx.doi.org/10.1007/978-3-658-22209-3.

Künneke, T. and Zimmer, D. (2017), "Funktionsintegration additiv gefertigter Dämpfungsstrukturen bei Biegeschwingungen", in Richard, H.A., Schramm, B. and Zipsner, T. (Eds.), Additive Fertigung von Bauteilen und Strukturen, Springer Fachmedien Wiesbaden, Wiesbaden, pp. 61–74. http://dx.doi.org/10.1007/978-3-658-17780-5_4.

Künneke, T. and Zimmer, D. (2021), "Konstruktionsregeln für additiv gefertigte Partikeldämpfer/Design rules for additive manufactured particle dampers", Konstruktion, Vol. 73 No. 11-12, pp. 72–78. http://dx.doi.org/10.37544/0720-5953-2021-11-12-72.

Lachmayer, R., Gembarski, P.C., Gottwald, P. and Lippert, R.B. (2017), "The Potential of Product Customization Using Technologies of Additive Manufacturing", in Bellemare, J., Carrier, S., Nielsen, K. and Piller, F.T. (Eds.), Managing Complexity, Springer Proceedings in Business and Economics, Springer International Publishing, Cham, pp. 71–81. http://dx.doi.org/10.1007/978-3-319-29058-4_6.

Lachmayer, R. and Lippert, R.B. (2020), Entwicklungsmethodik für die Additive Fertigung, Springer Berlin Heidelberg, Berlin, Heidelberg. http://dx.doi.org/10.1007/978-3-662-59789-7.

Lu, Z., Wang, Z., Masri, S.F. and Lu, X. (2017), "Particle impact dampers: Past, present, and future", Structural Control and Health Monitoring, Vol. 25 No. 1, e2058. http://dx.doi.org/10.1002/stc.2058.

Papalou, A. and Masri, S.F. (1996), "Performance of Particle Dampers Under Random Excitation", Journal of Sound and Vibration, Vol. 118 No. 4, pp. 614–621. http://dx.doi.org/10.1115/1.2888343.

Reiher, T. (2019), "Intelligente Optimierung von Produktgeometrien für die additive Fertigung", Dissertation, Shaker Verlag, 2019.

Saeki, M. (2005), "Analytical study of multi-particle damping", Journal of Sound and Vibration, Vol. 281 No. 3-5, pp. 1133–1144. http://dx.doi.org/10.1016/j.jsv.2004.02.034.

Schmitz, T., Gomez, M., Ray, B., Heikkenen, E., Sisco, K., Haines, M. and Osborne, J.S. (2020), "Damping and mode shape modification for additively manufactured walls with captured powder", Precision Engineering, Vol. 66, pp. 110–124. http://dx.doi.org/10.1016/j.precisioneng.2020.07.002.

Scott-Emuakpor, O., Beck, J., Runyon, B. and George, T. (2021), "Determining unfused powder threshold for optimal inherent damping with additive manufacturing", Additive Manufacturing, Vol. 38, p. 101739. http://dx.doi.org/10.1016/j.addma.2020.101739.

Scott-Emuakpor, O., George, T., Runyon, B., Holycross, C., Langley, B., Sheridan, L., O'Hara, R., Johnson, P. and Beck, J. (2018), "Investigating Damping Performance of Laser Powder Bed Fused Components With Unique Internal Structures", in Volume 7C: Structures and Dynamics, V07CT35A020. http://dx.doi.org/10.1115/GT2018-75977.

Scott-Emuakpor, O., George, T., Runyon, B., Langley, B., Sheridan, L., Holycross, C., O'Hara, R. and Johnson, P. (2019), "Forced-Response Verification of the Inherent Damping in Additive Manufactured Specimens", in Kramer, S., Jordan, J.L., Jin, H., Carroll, J. and Beese, A.M. (Eds.), Mechanics of Additive and Advanced Manufacturing, Volume 8, Conference Proceedings of the Society for Experimental Mechanics Series, Vol. 264, Springer International Publishing, Cham, pp. 81–86. http://dx.doi.org/10.1007/978-3-319-95083-9_15.

Wiberg, A., Persson, J. and Ölvander, J. (2019), "Design for additive manufacturing – a review of available design methods and software", Rapid Prototyping Journal, Vol. 25 No. 6, pp. 1080–1094. http://dx.doi.org/10.1108/RPJ-10-2018-0262.

Wurst, J., Schneider, J.A., Ehlers, T., Mozgova, I. and Lachmayer, R. (2022), "Corporate Strategy Based Quantitative Assessment of Sustainability Indicators at the Example of a Laser Powder Bed Fusion Process", in Scholz, S.G., Howlett, R.J. and Setchi, R. (Eds.), Sustainable Design and Manufacturing, Smart Innovation, Systems and Technologies, Vol. 262, Springer Singapore, Singapore, pp. 34–44. http://dx.doi.org/10.1007/978-981-16-6128-0_4.

Yang, S., Tang, Y. and Zhao, Y.F. (2015), "A new part consolidation method to embrace the design freedom of additive manufacturing", Journal of Manufacturing Processes, Vol. 20, pp. 444–449. http://dx.doi.org/10.1016/j.jmapro.2015.06.024.